Surface Science 605 (2011) 1263–1270

Contents lists available at ScienceDirect

Surface Science

journal homepage: www.elsevier.com/ locate/susc

Noble-metal nanostructures on carburized W(110)

Magdalena Bachmann [1], Norbert Memmel *, Erminald Bertel

Institute of Physical Chemistry, University of Innsbruck, Innrain 52a, 6020 Innsbruck, Austria

ARTICLE INFO

Article history:
Received 23 December 2010
Accepted 7 April 2011
Available online 14 April 2011

Keywords:
Tungsten
Carbon
Nanostructures
Gold
Silver
Copper

ABSTRACT

Noble metal nanostructures of Au, Ag and Cu were prepared on two types of carbon-modified W(110) surfaces—R(15×12) and R(15×3)—and investigated by means of scanning tunneling microscopy. For all deposited metals qualitatively the same behaviour is observed: On the R(15×12)-template always isotropic clusters are formed. In contrast, on the R(15×3)-substrate the anisotropy of the nanostructures can be tuned from clusters at low temperatures via thin nanowires to thicker nanobars at high deposition temperatures. At intermediate temperatures on the R(15×3) the anisotropic Au nanowires arrange themselves into straight lines along domain boundaries induced by deposition of the Au metal. Similarities and differences to Au nanostructures as recently reported by Varykhalov et al. [A. Varykhalov, O. Rader, W. Gudat. Physical Review B 77, 035412 (2008).] are discussed.

1. Introduction

In the last few years, fabrication of nanostructures has become a subject of tremendous interest. An intriguing aspect of nanostructures is related to their properties, which often differ drastically from those of the bulk material. One of the most impressive examples for altered properties with decreasing size is the catalytic behaviour of small gold particles: Albeit known for its inert nature in bulk state, gold—if reduced to a size in the range of a few nanometers—exhibits a surprisingly high activity and selectivity for a variety of oxidation reactions [2]. The origin of this unexpected reactivity, which was observed in case of other noble metals such as silver and copper as well [3], is discussed rather controversially—especially the role of the support material is still not clear at all [4–14]. Thus, there is a need for novel templates with different properties for the controlled growth of nano-sized objects. Comparing the catalytic activity of the particles on different substrates will then allow to find out to what extend cluster-support interactions determine the catalytic performance.

We have recently shown, that the carbon-induced R(15×12)-overstructure on W(110) serves as a well-suited template for the growth of regularly sized monolayer-high Ag and Co nanodots, preferentially consisting of ≈7 atoms [15]. These clusters are arranged in lines on an anisotropic grid. To produce such highly ordered chains of clusters, we followed the well-established route of deposition on a pre-structured substrate which provides preferential nucleation sites (as given by lattice dislocations, moiré patterns, surface reconstructions etc.), thus determining the arrangement of deposited atoms. In case of the system we used, carbon-rich regions of the template unit cell are unfavourable for metal adsorption, thus limiting cluster growth to the tungsten-rich areas of the unit cell. Due to the anisotropic size of the unit cell (1.37 nm×3.10 nm) quasi-one dimensional cluster arrays ("chains") are formed, aligned along the $\langle 1\,\bar{1}\,1\rangle$ directions.

Varykhalov et al. demonstrated that it is possible to grow Au clusters on a different carbon overstructure, the R(15×3)C/W(110), as well. In contrast to deposition on the R(15×12)-template, these clusters are larger and two monolayers high.[1] Results obtained by this group on Au-cluster growth on the R(15×12)C/W(110) template, however, revealed remarkable differences to our results: Besides less regular cluster growth, different cluster sizes and cluster distances, an alignment of the Au clusters in $[\bar{1}\,12]$ direction is reported in Ref. [1], which is perpendicular to the Ag and Co cluster chains we observed.

Currently it is unclear, if these differences are due to the use of different deposition materials (Au vs. Ag/Co), different deposition temperatures (room-temperature vs. 500 K–700 K) or different protocols for preparation of the R(15×12)C/W(110) substrate (i.e. different carbon-containing feed gases, different cracking temperatures and different post-cracking annealing temperatures). In order to illuminate the origin of these discrepancies and to obtain a broader perspective for the use of carburized W(110) surfaces as highly promising templates for catalytic applications, we systematically vary these parameters. We demonstrate that—as proposed in our previous work[15]—the R(15×12)C-superstructure serves as an universal template for regularly sized and regularly spaced nanoclusters not only for Ag and Co, but also for Cu and Au. The main difference to the work of Varykhalov et al.[1] is traced back to the omission of the post-cracking high-temperature anneal in Ref.[15]. With respect to growth

* Corresponding author. Tel.: +43 512 507 5073; fax: +43 512 507 2925.
E-mail address: norbert.memmel@uibk.ac.at (N. Memmel).
[1] Recipient of a DOC-fFORTE-fellowship of the Austrian Academy of Sciences at the Institute for Physical Chemistry.

0039-6028
doi:10.1016/j.susc.2011.04.013

on the R(15×3)-template we verify the findings of Varykhalov et al. for Au deposition and show that similar cluster-structures can be created with Cu and Ag as well if the template is cooled to below room-temperature. In contrast, if deposition is carried out at elevated temperatures, we show that Cu, Ag and Au nanowires can be generated.

2. Experiment

Experiments were carried out in an UHV-system with a base pressure of 2×10^{-10} mbar, equipped with a DME (Danish Micro Engineering) room-temperature scanning tunneling microscope (STM). The W(110) surface was cleaned by flashing up to 2300 K and annealing at 1750 K in 5×10^{-8} mbar O_2. Starting from the clean surface, the standard procedure for preparation of the R(15×12)C/W(110) template was thermolysis of ethene at 1200 K–1700 K, followed by two short flashes up to 2400 K and rapid cooling. In order to compare to the experiments performed by Varykhalov et. al[1], we also followed their preparation procedure. In particular we examined substituting ethene with propylene and omitting the final flashes after deposition of carbon. The thermodynamically stable R(15×3)-substrate was routinely generated by deposition of ethene at 1200 K–1700 K and subsequent annealing in vacuum at ≈1700 K.

Au and Ag were evaporated from resistively heated alumina crucibles, Cu was deposited via electron-beam evaporation. Cu ions produced by the electron-beam were electrostatically deflected out of the deposition beam. Deposition rates of 0.05 ML up to 0.20 ML per minute were used (1 ML = 1 monolayer = 1.4×10^{15} atoms/cm^2). Coverages were deduced from deposition time and calibrated by STM images of extended metal islands on clean W(110).

3. Results and discussion

3.1. Deposition of noble metals on R(15x12)C/W(110)

Commonly R(15×12)C/W(110) surfaces show a characteristic STM pattern with bright protrusions bridged by two smaller ones (Fig. 1a).[1,15,16]. Due to the large unit cell (1.37 nm×3.10 nm) equivalent to 60 W atoms, the exact atomic configuration has not been determined so far. According to the interpretation of atomically resolved details[16], the bright areas are attributed to tungsten-rich regions of the unit cell. However, it has to be mentioned, that the structure's appearance is quite sensitive to tip condition and tunneling parameters, so that the larger maxima might appear as dark holes as well.[15] Hence, in order to avoid confusion, we will

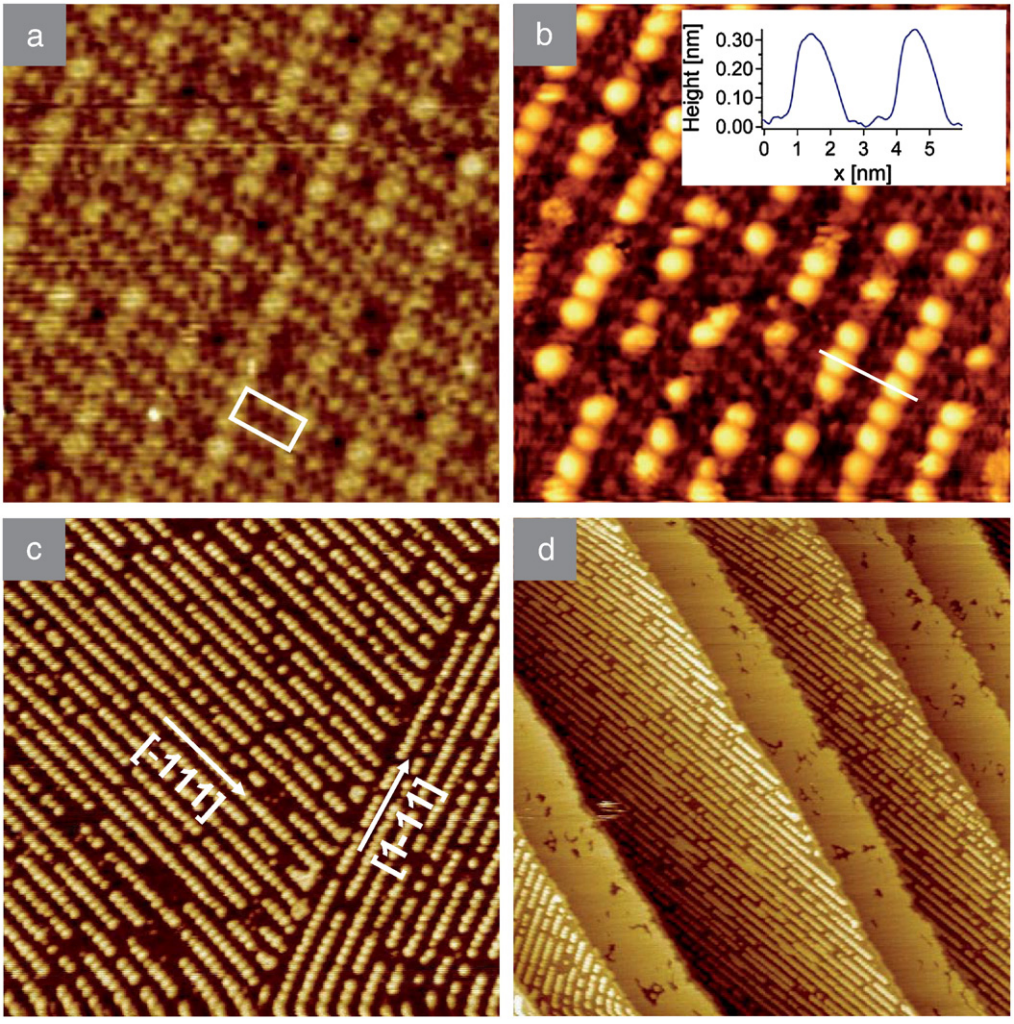

Fig. 1. Increasing amounts of Au on R(15×12)C/W(110) at 700 K. (a) Clean R(15×12)C/W(110) template. Due to thermal drifting the rectangular unit cell appears slightly oblique. (b) Low coverage experiment (<0.12 ML) for determination of the nucleation site. A clearly resolved carbon overstructure (note protruding maxima between the Au clusters) enables unambiguous identification of the adsorption area: Nucleation of Au nanodots is preferred in the carbon poor regions of the unit cell. (c) Regular cluster growth at optimized preparation conditions (local coverage: 0.12 ML). (d) Transport of Au atoms in "excess" of 0,12 ML from carbon-modified patches to clean W(110) terraces. Image sizes: (a) 21 nm×21 nm, (b) 24 nm×24 nm, (c) 80 nm×80 nm, (d) 160 nm×160 nm.

refer in the following to the two smaller bridging maxima which are rather insensitive to tunneling conditions.

As described in Ref. [15], carbon diffusion from the surface to the bulk occurs preferentially at terrace edges. As a consequence, narrow terraces deplete faster in carbon than wider ones, resulting in coexisting narrow clean W terraces and broader carbon-modified ones.

Deposition of metals on the surface at elevated temperatures yields uniformly sized clusters, which are arranged on a rectangular grid defined by the lattice of the underlying carbon superstructure. In case of Ag 500 K are sufficient to obtain perfectly aligned nanodot arrays[15], whereas for Au nanodots of a similar quality, the deposition temperature has to be elevated to 700 K, loosely following the trend expected from the melting temperatures of both materials (Ag 1234 K, Au 1337 K). As it has been observed for Ag and Co, Au nanoparticles nucleate on a rectangular grid with a cluster-cluster distance of 1.4 nm and 3.1 nm, respectively. Fig. 1b shows an STM image of Au clusters grown at 700 K. The underlying C-superstructure with its typical appearance is clearly visible, so that the nucleation site can again be assigned to those regions of the unit cell which we consider to be nearly unperturbed by carbon. Due to the resolved carbon-overstructure the directions of the underlying tungsten substrate can be identified unambiguously: The short axes of the (15×12) unit cell run either along $[1\,\bar{1}\,1]$ or the symmetry-equivalent $[\bar{1}\,1\,1]$ direction. Consequently, close to the optimum coverage (0.12 ML), lines of clusters ("chains") running along these directions are observed (Fig. 1c).

If more material is deposited at elevated temperatures, as shown in Fig. 1d, a similar scenario is observed as in case of Ag: Broader, carbon-modified terraces exhibit a very regular cluster growth, whereas on narrow carbon-free tungsten terraces nearly complete Au layers are formed. Two explanations of this observation are at hand: Either Au atoms in excess of the optimum coverage (which are only loosely bound to carbon-rich regions between the cluster rows) exhibit a very high mobility, resulting in diffusion of these atoms to clean tungsten terraces where adsorption is more favourable. Alternatively, this observation might be explained by a significant reduction of the sticking coefficient with increasing coverage on carbon-modified terraces. The latter scenario has not been considered so far. To discriminate between both explanations, the Au content on the surface was followed by Auger-electron spectroscopy (AES) on both clean W(110) and R(15×12)C/W(110) (see Fig. 2). Both data sets are virtually identical, thus excluding the latter scenario of a reduced sticking coefficient, as AES averages over macroscopic areas. However, large area STM images of 0,3 ML Au deposited onto a well-prepared R(15×12)C/W(110), free of narrow clean W terraces within the scan range of 1 μm^2, only show the STM pattern similar to Fig. 1c, typical for a coverage of ≈0.12 ML. This implies a very high mobility of Au atoms in excess, allowing diffusion across distances of more than 1 μm. In summary the experiments demonstrate unambiguously that—as expected from our previous work[15], but in contrast to Varykhalov et al.[1]—deposition of Au onto R(15×12)C/W(110) leads to the same type of structures as already observed for Ag and Co. In order to clarify if this discrepancy is caused by different deposition temperature (700 K in the present work vs. room-temperature in Ref.[1]), deposition studies at room-temperature and below were carried out as well. As can clearly be seen from Fig. 3a and b, decreasing deposition temperature leads to increasing disorder of the clusters and a broader size distribution. However, the preferential orientation of the cluster chains along the $[1\,\bar{1}\,1]$ and $[\bar{1}\,1\,1]$ direction, respectively, is still discernible—in contrast to images observed by Varykhalov and co-workers. Hence, a strong discrepancy in room-temperature cluster growth between the present work and Ref. [1] is ascertained and has to be discussed. As the type of deposited metal as well as the deposition temperature are not responsible for the observed differences, they obviously are related to different preparation protocols for the R(15×12)-template.

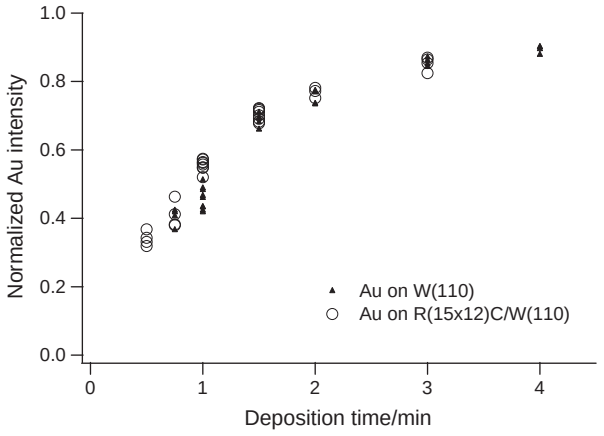

Fig. 2. Normalized AES-Signal vs. deposition time for Au on R(15×12)C/W(110) and Au on W(110) at 700 K. Reduction of the sticking coefficient on carbon-modified patches of the surface can be excluded due to the same amount of Au on both surfaces.

There are three main differences concerning the fabrication of the carbon overstructure: (1) Different hydrocarbons were used for deposition of carbon onto the W(110) substrate—in Ref. [1] propylene was thermally cracked, whereas in the present work ethene was applied to generate the R(15×12)C/W(110) overstructure. (2) Slight deviations in cracking temperature, i.e. substrate temperature during gas exposure, exist: As described by Varykhalov et al., the crystal was exposed to the gas at 1000 K–1100 K[1], whereas we heated the sample up to 1300 K–1700 K. (3) R(15×12)C/W(110) commonly is produced by flashing R(15×3)C/W(110) to 2300 K–2600 K, followed by rapid cooling [17,18], which is also the method we used for generation of our template. This final step of the preparation method was avoided in the study described in Ref. [1].

Ethene and propylene gas, respectively, merely serves as a carbon supply. Both gases exhibit a high degree of analogy (both are hydrocarbons and contain a π-bonding for facilitated adsorption). Furthermore, as reported by Rawlings et al. [19], it is possible to modify W(110) with carbon by cracking acetylene as well, implying that the type of carbon-containing gas is not relevant. Nevertheless, to rule out any influences which might be induced by different gases, we replaced ethene by propylene. Starting from a clean W(110) surface, a LEED (Low-Energy Electron-Diffraction) investigation in course of successive exposure to propylene at 1000 to 1100 K did not show any characteristic (15×12)-spots which normally occur additionally to the (15×3)-spots. The LEED-pattern obtained from this preparation method more resembles the (15×3)-pattern although the LEED-spots are less well-defined than in case of gas exposure at higher temperatures, indicating worse ordering. Deposition of Au onto such a surface at room-temperature yields cluster structures which exhibit a broad size distribution and no special ordering, as pictured in Fig. 3c. Images with partially resolved carbon overstructure reveal no large homogeneous domains, but rather very small (15×3)-patches containing just a few unit cells (see Fig. 3d).

However, if this (15×3)-like structure is flashed several times to about 2400 K, followed by deposition of Au at 700 K, highly ordered cluster arrays aligned in $[1\,\bar{1}\,1]$ and $[\bar{1}\,1\,1]$ direction are obtained as in case of our standard preparation method. This clearly indicates, that the final flash is indeed the most critical step to fabricate a perfect R(15×12)C/W(110) surface: Besides better ordering due to higher temperature, the final anneal drives excess carbon into the bulk, thus defining the correct surface carbon concentration for the (15×12)-structure. Note that in addition rapid cooling of the crystal is essential to "freeze" the carbon concentration on the surface and to avoid (back-)segregation of carbon from the bulk. Hence, it is reasonable to assume that the different and less regular ordering observed in Ref. [1]

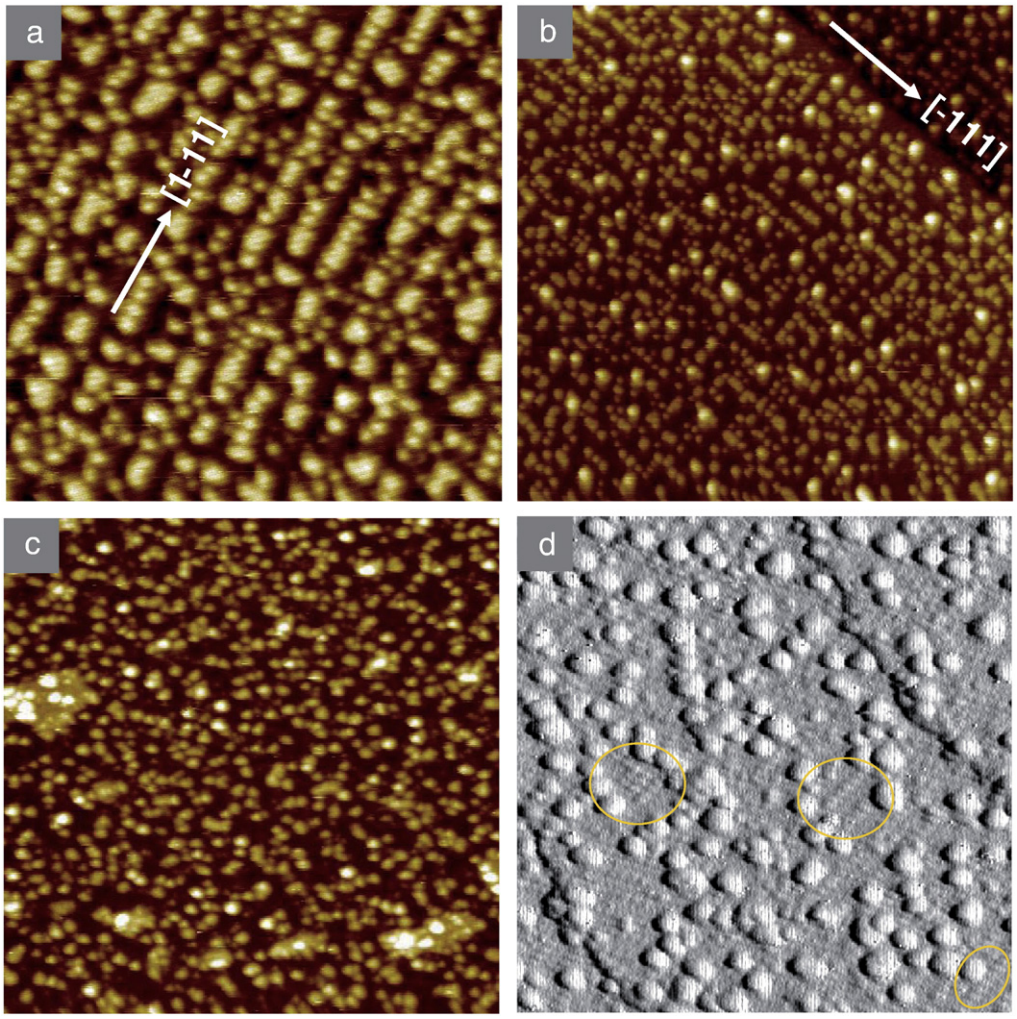

Fig. 3. Au deposited on differently prepared C/W(110) structures. Deposition of Au at room-temperature (a) and after cooling with liquid nitrogen (b) leads to a loss of uniformity, even though the preferred orientation is still visible. Preparation of the sample following the route as proposed in Ref. [1] results in no special ordering of the nanodots (c). Replacing propylene with ethene yields a similar picture (d). Note the small resolved patches with (15×3) unit cells indicating a quite inhomogeneous carbon-modification. Image sizes: (a) and (d) 40 nm×40 nm; (b) and (c) 80 nm×80 nm.

is due to an inhomogeneous carbon modification of the W(110). We would like to note that production of a perfect (15×12)-superstructure is quite elaborate due to a strong dependence on the carbon concentration in the bulk. Thus, an exact reproduction of previous results is only possible, if the history of the sample is known.

With regard to prospective investigations of the catalytic properties of nanoparticles on carburized W(110), the growth of copper clusters on R(15×12)C/W(110) was studied as well. Perfectly arranged nanodot arrays can be observed for deposition at 700 K, which is again consistent with the trend expected from the melting point (1358 K) (see Fig. 4d). Low coverage images with resolved carbon-overstructure allow identification of the nucleation site of the clusters, which is—as in case of the other metals—restricted to carbon-poor areas of the unit cell, resulting also in a narrow size distribution (see Fig. 4a). Close to the interface (usually steps) to carbon-free terraces, relatively wide zones depleted in Cu clusters are observed (Fig. 4b). If the local fraction of clean W(110) areas surrounding a (15×12)-region is high enough, even the whole (15×12)-area might be free of Cu (see right hand terrace in Fig. 4c). Such denuded areas were only barely visible for Ag and Au, indicating a weaker bonding or lower migration barrier out of the nucleation area for Cu on R(15×12)C/W(110). The existence of denuded zones also provides further evidence that transport to carbon-free terraces rather than a reduction of the sticking coefficient is responsible for the "disappearance" of deposited material in some STM images for coverages beyond the optimum coverage (c.f. AES measurements for deposition of Au, Fig. 2).

3.2. Deposition of noble metals on R(15×3)C/W(110)

In Fig. 5 the evolution of Au nanostructures on the R(15×3)-template with increasing deposition temperature is displayed. In accordance with the results of Varykhalov et al.[1] deposition of Au at room-temperature leads to the formation of nano-sized clusters (Fig. 5a). On the uncovered parts of the underlying template faint protruding stripes, running along $[1\,\bar{1}\,2]$ are visible. These stripes have a distance of 1.37 nm and indicate the direction of the short axis of the (15×3) unit cell (for a schematic of the (15×3) unit cell see inset in Fig. 6). A close-up view shows, that along $[1\,\bar{1}\,2]$ these stripes exhibit a weak corrugation with a periodicity of 0.8 nm, which is the length of the short (15×3) unit cell axis. In the following we will refer to the region between two neighboring stripes as the "rows" of the (15×3)-phase. The Au clusters of Fig. 5a are always located inside an individual row, in full agreement with the observations of Varykhalov and co-workers. This also implies that the width of the clusters along $[-1\,1\,1]$ is less than the width of a single row (1.37 nm). The height of

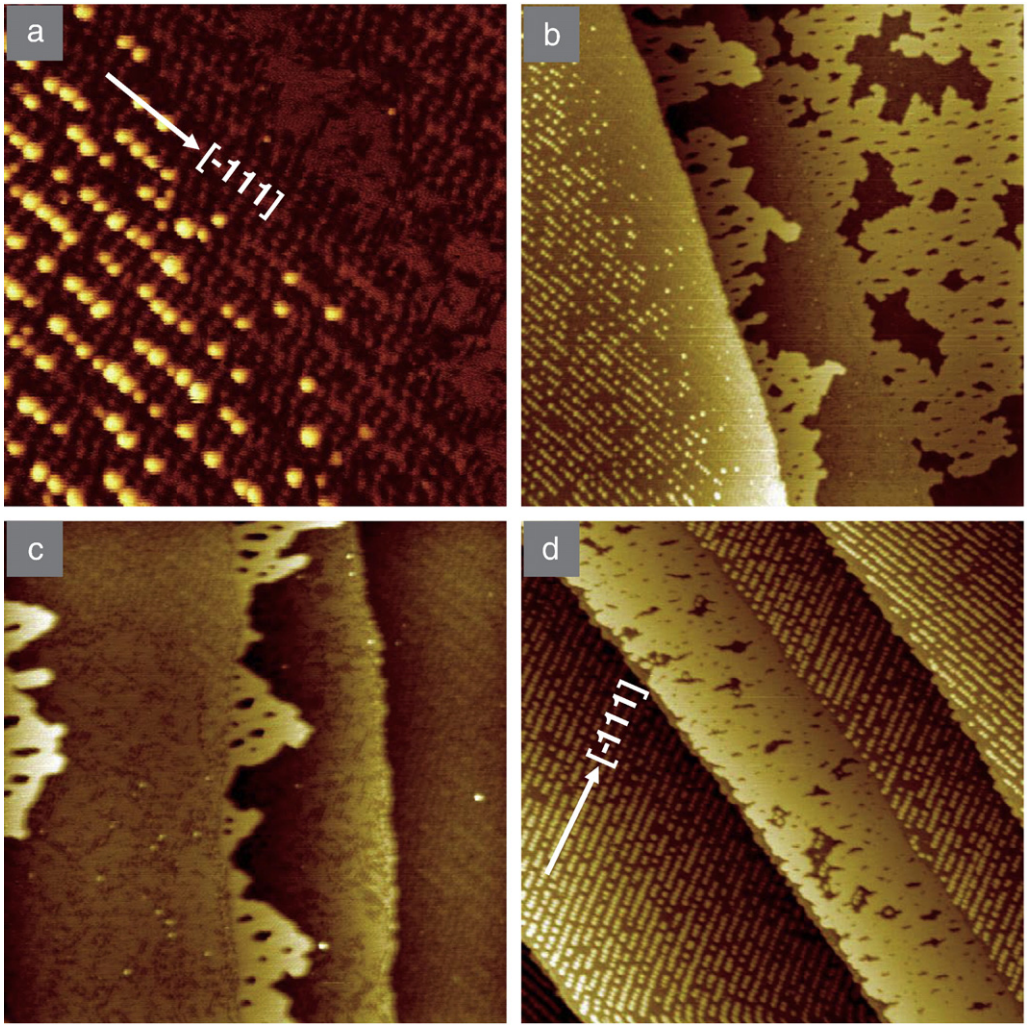

Fig. 4. Copper on R(15×12)C/W(110) deposited at 700 K. Resolution of typical features of the template overstructure permits identification of the nucleation sites of the clusters which are situated in the tungsten-rich patches of the unit cell (a). Note the large area on the terrace not covered with the carbon superstructure, resulting in a strong depletion in Cu in adjacent boundary regions. This effect is even more prominent in (b): Large "clean" W(110) areas, adjacent to (15×12)-patches, cause a decrease in cluster density at terrace edges. If the local fraction of W(110) is large enough to receive the hole amount of Cu deposited, carbon-modified regions completely deplete in Cu, as it can be seen for example in the right-hand terrace of image (c). If less clean tungsten terraces are available (d), similar results are obtained as for Au: Carburized regions exhibit a regular cluster growth, whereas "clean" W-terraces are nearly entirely filled with Cu monolayers. Image sizes: (a) 40 nm×40 nm; (b) and (d) 160 nm×160 nm; (c) 80 nm×80 nm.

most of the clusters amounts to ≈0.45 nm. This is about twice the distance between Au(111) planes (236 pm). Hence, in accordance with Varykhlaov et al., we assign the observed structures to clusters of double-layer height.

After deposition at 500 K, the clusters are aligned in lines running along $[1\bar{1}2]$ (Fig. 5b). Clusters in neighbouring rows are hardly observed, implying that at 500 K Au atoms can easily migrate from one row to the next. Simultaneously the width of the clusters perpendicular to the rows starts to exceed the width of a single (15×3)-row. In contrast, the height of the majority of the clusters remains nearly unchanged, i.e. the clusters are still of double-layer height.

The most obvious change upon increasing the temperature to 650 K is the altered particle shape: Now elongated anisotropic islands are formed, more resembling disrupted wires than clusters (Fig. 5c). The preferred orientation is along the direction of the (15×3)-rows. Perpendicular to the rows the islands width is limited to the width of two (15×3)-rows, i.e. ≈2.8 nm. The height of most of the structures is about 0.5 nm, i.e. two monolayers as in case of the clusters generated at lower temperatures. A particular intriguing feature of Fig. 5b and c is the alignment of the grown structures into straight lines with "empty" regions in between the lines. Due to this ordered arrangement it seems clear that the pattern is not controlled by kinetics. In such a case a more random distribution would be expected. Rather this line-like ordering implies a kind of attractive interactions between neighbouring structures in the same (15×3)-row. The clue to the explanation of this one-dimensional arrangement comes from inspection of line profiles perpendicular to the rows of clusters/wires in images with resolved (15×3)-overstructure as displayed in Fig. 6. On the bare terraces to the left and right of the nanostructure, the 1.37 nm periodicity of the (15×3)-structure can nicely be recognized. However, the overstructures on both sides of the nanostructure are not in registry with each other. Rather they are shifted in relation to each other by ≈ 1/5 of the width of a (15×3)-row, i.e. by one atomic distance of the underlying W(110) substrate along $[\bar{1}11]$ (see inset in Fig. 6). Thus it is clear that the one-dimensional arrangement is due to decoration of "antiphase" domain boundaries of the (15×3)-overlayer (more precisely the phase shift is $2\pi/5$). However, despite careful searching, such domain boundaries were never observed for the pure (15×3)-template. Hence we conclude, that the domain boundaries are induced by the deposited Au material. This also explains why the nanowires are only observed at elevated temperatures (>500 K). At lower temperatures the thermal energy is not sufficient to allow a rearrangement of the

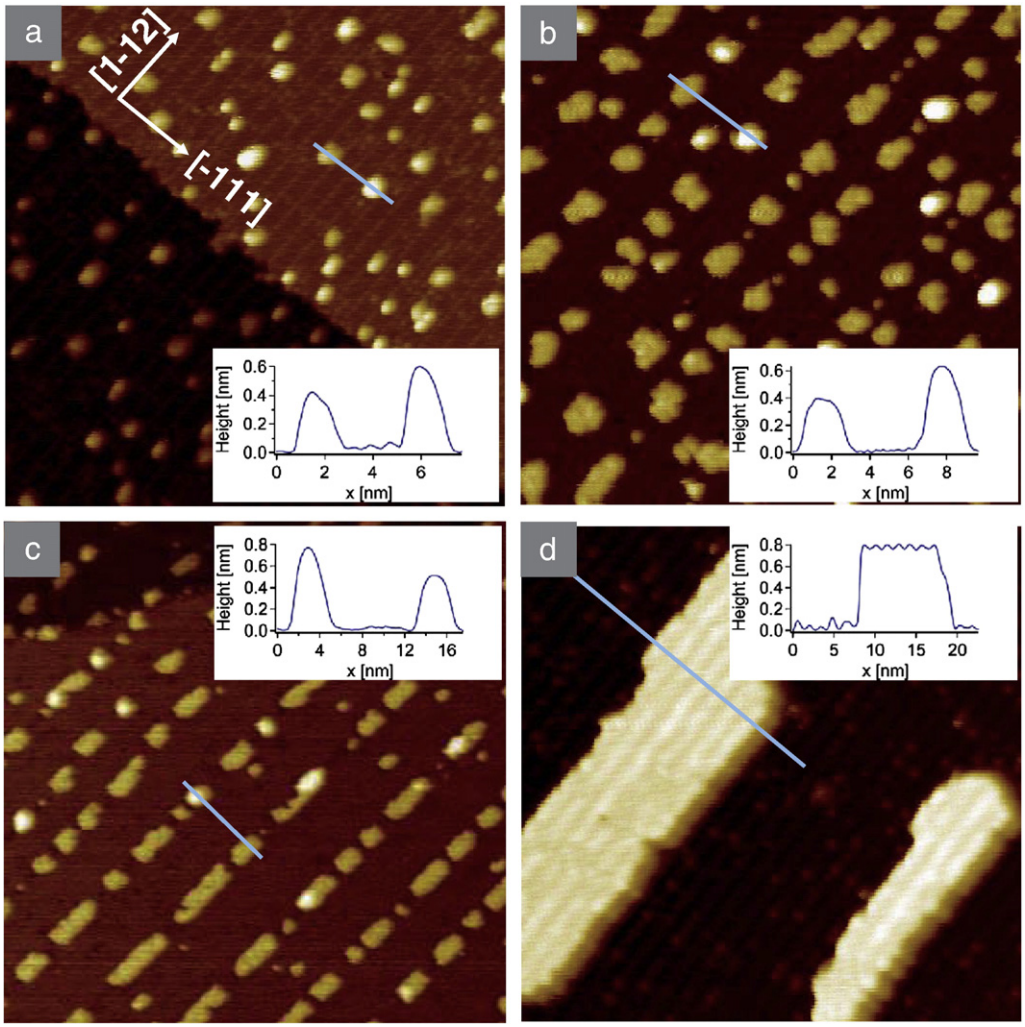

Fig. 5. Au on R(15×3)C/W(110) deposited at room-temperature (a), ≈500 K (b), ≈650 K (c) and ≈750 K (d). Image sizes: (a), (b) 40 nm×40 nm; (c) 80 nm×80 nm; and (d) 35 nm×35 nm.

template structure and insertion of domain boundaries. However, insertion of a single "antiphase" domain boundary into a single domain structure is difficult to accomplish, as it requires a shift of the template overstructure on one-half of the entire surface and thus involves macroscopic mass-transport. In order to avoid such a macroscopic mass-transport, domain boundaries are expected to form as closed loops. In this case only the template structure within the enclosed area has to be rearranged. In the present case these loops are formed by neighbouring parallel domain boundaries which are connected to each other at terrace steps crossing the (15×3)-rows. As a consequence we conclude that the parallel domain boundary lines observed in the experiment always form in pairs. This necessarily implies some effective interaction between neighbouring domain boundary lines. We propose that this interaction is responsible for the quite regular distance between the lines of nanoclusters/-wires as observed in our experiment.

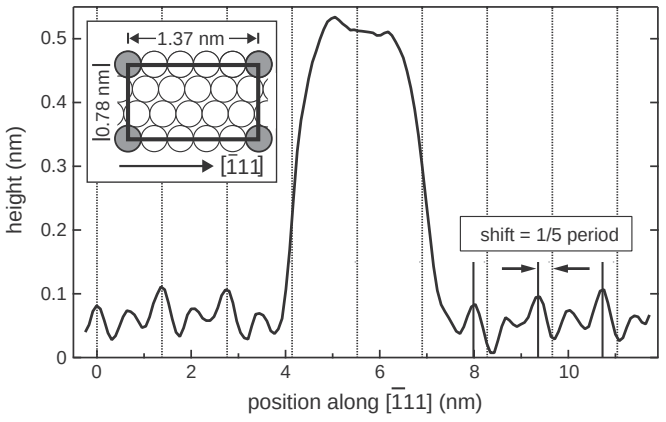

Fig. 6. Line profile perpendicular to the Au-nanowires observed at a deposition temperature of 650 K. The (15×3)-units on both sides of the nanowire are out of registry, indicating the existence of a 2π/5-domain boundary underneath the nanowire. Inset: Schematic of the (15×3) unit cell size relative to the W(110) substrate.

Finally we note that in the room-temperature deposition experiment of Varykhalov et al. such lines of clusters were also occasionally observed (Fig. 2d of Ref.[1]). A detailed inspection of the corrugation pattern across these lines reveals that—exactly as in our study—antiphase domain boundaries are hidden underneath these cluster lines. However, as large-area scans of the bare (15×3)-template are not available, it is not clear, if these underlying domain boundaries were already present on the bare template or if they were induced by metal deposition.

Deposition of Au at 750 K yields larger "bar"-like anisotropic structures, again directed along [1$\bar{1}$2] or [$\bar{1}$12], respectively (Fig. 5d). In contrast to the wire-like structures at 650 K the width of the bars is not restricted to two(15×3)-rows, but can be considerably larger. As

it is evident from the line profile in the inset of Fig. 5d, the bars are also higher (≈0.8 nm), indicating a trend for preferred agglomeration into more than double-monolayer high structures, as to a small extent already observed at 500 K and 650 K. Interestingly, the flat tops of those bars exhibit the same 1.37 nm periodicity as the rows of the underlying (15×3)-substrate. The (15×3)-rows on both sides of these nanobars are in registry with each other, implying that either the Au-induced domain boundaries are unfavourable underneath such wider and thicker Au nanobars or that smaller domain-boundary loops have formed which are hidden underneath the Au nanobars, most presumably along the rim of these structures.

The main results on Au growth on R(15×3)C/W(110) can be summarized as follows: Upon submonolayer deposition, nanostructures are formed which can be tuned from small nm-sized, double-layer clusters at room-temperature to nanowires/-bars of different widths and heights by increasing the temperature. A similar trend is also observed in case of Cu and Ag deposition (Fig. 7). In contrast to gold, nanowires of Cu are already formed at room-temperature. The Cu nanowires of Fig. 7b resemble the Au nanowires formed at 650 K, while—due to the elevated deposition temperature of 500 K—the Ag nanostructures of Fig. 7d are basically replicas of the Au nanobars observed after deposition at 750 K. Ag nanostructures with lengths up to 300 nm were observed. Accordingly, to grow Cu and Ag clusters, it is necessary to cool the sample to below room-temperature (Fig. 7a and b). Similar to the case of gold, the width of such-prepared Cu and Ag clusters is about equal to the width of a single (15×3)-row, i.e. 1.4 nm. However, their height is larger (≥0.6 nm), thus the particles are probably three layers in height.

Formation of (gold) nanowires on (15×3)C/W(110) was already reported by Varykhalov et al.[20,21]. However, these nanowires were prepared by a different procedure, namely deposition at room-temperature with subsequent annealing to 870 K, and are of different origin: Their apparent height is only around 60 pm, they always appear in pairs with one continuous and one modulated wire and—most importantly—they are aligned close to the [0 0 1] direction of W(110), in contrast to the structures of the present work which run along [1 $\bar{1}$ 2] or [$\bar{1}$ 1 2], respectively, i.e. the direction of the (15×3)-rows. Varykhalov and co-workers attribute the nanowires formed by their preparation protocol to Au atoms embedded into the first (or even second) atomic plane of the (15×3)C/W(110) surface. In contrast, in the present study we do not have any indication for immersion of the noble metal structures (both clusters and wires/bars) into the underlying substrate, although creation of antiphase-domain boundaries in the (15×3)-template by deposition of Au at

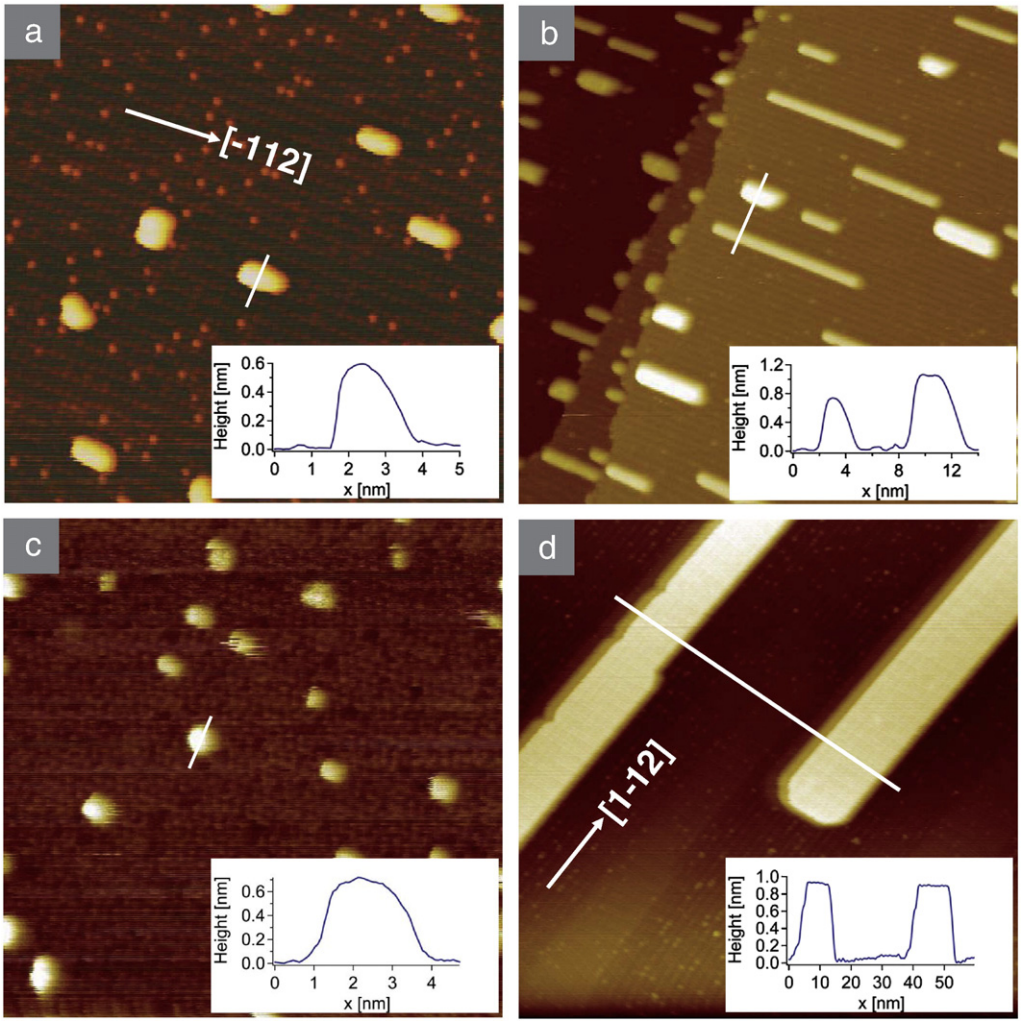

Fig. 7. Copper and Silver deposited on R(15×3)C/W(110) at variable temperatures. (a) Cu-deposition at low temperature (cooling of the sample with liquid nitrogen) yields small clusters with a height of 0.6 nm. (b) Cu deposited on the surface at room-temperature, resulting in nanowires with heights of 0.7 nm-1,1 nm (see inset). Note the resolved lines of the underlying superstructure which allow determination of the orientation of the W substrate. Ag exhibits a similar behaviour: Deposition onto the cooled crystal results in cluster growth (c), whereas at 500 K (d) larger nanowires are observed. Image sizes: (a) and (c) 40 nm×40 nm; (c) and (d) 80 nm×80 nm.

intermediate temperatures (500 K–650 K) shows that also in this case the substrate structure is not rigid but can be altered by the deposited metal.

4. Summary

We have shown that carburized W(110) surfaces serve as well-suited templates for the growth of tunable nanostructures. On the metastable R(15×12)C/W(110) very small (≈7 atoms), one-dimensionally arranged Au, Ag and Cu nanodots with a very narrow size distribution and monolayer height can be grown. Discrepancies to investigations published by Varykhalov et al. concerning the preferred orientation of the clusters are attributed unambiguously to the lack of final flashing to 2400 K in preparation of the (15×12)-superstructure. On the thermodynamically stable R(15×3)C/W(110) template at low deposition temperature also clusters can be grown. In contrast to the 7-atom clusters on R(15×12)C/W(110) they are larger and of bilayer rather than monolayer height. As compact structures on the (15×3)-substrate form only at low temperatures, their growth obviously is due to kinetic limitations, whereas the high-temperature clusters on the (15×12)-substrate are attributed to thermodynamic equilibrium structures[22]. By increasing the deposition temperature, the clusters generated on the (15×3)-template can be tuned into anisotropic nanowires/-bars. Due to the tunability of size, shape and height of the nanostructures formed on carburized W(110), they exhibit high potential to explore the relation between size and catalytic activity of noble-metal particles. Measurements of these properties are on the way.

Acknowledgements

This work was carried out within the research platform Advanced Materials at the University of Innsbruck. Financial support by the Austrian Science Fund (FWF grant No. S9004-N20) as well as the Austrian Academy of Sciences is gratefully acknowledged.

References

[1] A. Varykhalov, O. Rader, W. Gudat, Phys. Rev. B 77 (2008) 035412.
[2] M. Haruta, T. Kobayashi, H. Sano, N. Yamada, Chem. Lett. 16 (1987) 405.
[3] M.J. Lippits, A.C. Gluhoi, B.E. Nieuwenhuys, Top. Catal. 44 (2007) 159.
[4] B.K. Min, C.M. Friend, Chem. Rev. 107 (2007) 2709.
[5] M. Valden, X. Lai, D.W. Goodman, Science 281 (1998) 1647.
[6] M.S. Chen, D.W. Goodman, Science 306 (2004) 252.
[7] M. Turner, V.B. Golovko, O.P.H. Vaughn, P. Abdulkin, A. Berenguer-Murcia, M.S. Tikhov, B.F.G. Johnson, R.M. Lambert, Nature 454 (2008) 981.
[8] B. Yoon, H. Häkkinen, U. Landman, A.S. Wörz, J.-M. Antonietti, S. Abbet, K. Judai, U. Heiz, Science 307 (2005) 403.
[9] A. Sanchez, S. Abbet, U. Heiz, W.-D. Schneider, H. Häkkinen, R.N. Barnett, U. Landman, J. Phys. Chem. A 103 (1999) 9573.
[10] U. Heiz, E.L. Bullock, J. Mater. Chem. 14 (2004) 564.
[11] C. Lemire, R. Meyer, S. Shaikhutdinov, H.-J. Freund, Angew. Chem. Int. Ed. 43 (2004) 118.
[12] C. Lemire, R. Meyer, S. Shaikhutdinov, H.-J. Freund, Surf. Sci. 552 (2004) 27.
[13] H. Falsig, B. Hvoelbæk, I.S. Kristensen, T. Jiang, T. Bligaard, C.H. Christensen, J.K. Nørskov, Angew. Chem. Int. Ed. 47 (2008) 4835.
[14] M. Comotti, W.-E. Li, B. Spliethoff, F. Schüth, J. Am. Chem. Soc. 128 (2006) 917.
[15] M. Bachmann, M. Gabl, C. Deisl, N. Memmel, E. Bertel, Phys. Rev. B 78 (2008) 235410.
[16] M. Bode, R. Pascal, R. Wiesendanger, Surf. Sci. 344 (1995) 185.
[17] E. Bauer, Surf. Sci. 7 (1967) 351.
[18] R. Baudoing, R.M. Stern, Surf. Sci. 10 (1968) 392.
[19] K.J. Rawlings, S.D. Foulias, B.J. Hopkins, J. Phys. C: Solid State Phys. 14 (1981) 5411.
[20] A. Varykhalov, O. Rader, W. Gudat, Phys. Rev. B 72 (2005) 115440.
[21] A. Varykhalov, C. Biswas, W. Gudat, O. Rader, Phys. Rev. B 74 (2006) 195420.
[22] M. Gabl, M. Bachmann, N. Memmel, E. Bertel, Phys. Rev. B 79 (2009) 153409.